CHINESE OPTICS LETTERS

Vol. 22, No. 3 | March 2024

LP modes exchange based on multiplane light conversion

Yanan Zhong (钟亚楠)[†], Chuxuan Lin (林楚璇)[†], Juncheng Fang (方浚丞)[**], Ting Lei (雷 霆), and Xiaocong Yuan (袁小聪)[*]

Nanophotonics Research Centre, Shenzhen Key Laboratory of Micro-Scale Optical Information Technology & Institute of Microscale Optoelectronics, Shenzhen University, Shenzhen 518060, China

[†]These authors contributed equally to this work.

*Corresponding author: xcyuan@szu.edu.cn

**Corresponding author: junchengfang@szu.edu.cn

Received October 11, 2023 | Accepted November 29, 2023 | Posted Online March 22, 2024

Data exchange between different mode channels is essential in the optical communication network with mode-division multiplexing (MDM). However, there are challenges in realizing mode exchange with low insert loss, low mode crosstalk, and high integration. Here, we designed and fabricated a mode exchange device based on multiplane light conversion (MPLC), which supports the transmission of LP01, LP11a, LP11b, and LP21 modes in the C-band and L-band. The simulated exchanged mode purities are greater than 85%. The phase masks were fabricated on a silicon substrate to facilitate the integration with optical systems, with an insert loss of less than 2.2 dB and mode crosstalk below −21 dB due primarily to machining inaccuracies and alignment errors. We carried out an optical communication experiment with 10 Gbit/s OOK and QPSK data transmission at the wavelength of 1550 nm and obtained excellent performance with the device. It paves the way for flexible data exchange as a building block in MDM optical communication networks.

Keywords: mode exchange; mode-division multiplexing; multiplane light conversion.
DOI: 10.3788/COL202422.030602

1. Introduction

The transmission capacity of single-mode optical fibers has nearly approached the Shannon limit[1]. In order to meet the demands of high-capacity communication networks, various multiplexing techniques have been proposed, such as wavelength-division multiplexing (WDM)[2–4], polarization-division multiplexing (PDM)[5], and spatial-division multiplexing (SDM)[6–9]. Over the past few decades, WDM has played an important role in mode-division multiplexing (MDM) technology based on few-mode fiber (FMF), which is a form of SDM and presents a promising solution to the capacity crisis. An MDM communication system contains orthogonal modes of different orders such as linearly polarized (LP)[10,11] and orbital angular momentum (OAM)[12–14] modes as independent channels within the FMFs. Recently, various devices for MDM communication systems have been proposed. These include mode multiplexers/demultiplexers (MMUXs/MDEMUXs), high-order mode fibers[8], mode-selective switches, and so on. MMUX/MDEMUX devices constitute the cornerstone of the MDM communication system and have been extensively researched. This encompasses various types of devices, including photonic-lantern-based multiplexers[15], waveguide devices[16], diffraction devices[17], liquid crystals[18], and so on. The data exchange between different channels is an indispensable function in the optical communication network. The traditional mode exchange approach initially demultiplexes multiple orthogonal mode lights into fundamental mode lights, performs mode exchange, and then remultiplexes using an MMUX, which involves multiple devices with a wide footprint and is inconsistent with the trend toward photonic integration. Therefore, it is necessary to propose an integrated mode exchange device. In addition, the integrated mode exchange device can be employed to balance the differential mode delay (DMD) in the long-distance optical fiber communication. DMD is defined as the relative delay of the transmission between mode groups[19]. The increase in DMD leads to a degradation in communication quality, accompanied by an elevation in the complexity of MIMO-DSP at the receiver. The data exchange between different mode groups is an effective solution for reducing the computational cost and minimizing system power consumption. For the device, the number of modes supported, conversion efficiency, and miniaturization are essential concerns. The mode exchange devices based on a silicon metastructure that achieved high conversion efficiencies have been reported[20].

Diffractive optical elements are phase components that generate the desired optical field through interference and diffraction. Metasurface is a technology for achieving efficient phase

shift[21]. By combining a metasurface on top of a planar waveguide, efficient conversion between TM and TE modes is achieved with 98% analog mode purity[22]. The researchers combined volume holograms with a random optical diffuser, and low crosstalk mode exchange was obtained[23]. However, the multiple quantity modes and the miniaturization cannot be fulfilled at the same time. Multiplane light conversion (MPLC) devices that utilize a multi-layer diffraction structure composed of multiple phase planes to modulate the input light field were proposed by researchers from CaiLabs in 2014. The MPLC devices have a high degree of freedom in wavefront modulation and demonstrate a unique advantage in mode control[24–27]. In the last few years, low-loss, broadband, and highly mode-selective MMUXs/MDEMUXs based on MPLC have been proposed[26,28]. It is possible to optimize a mode exchange device with low-mode crosstalk and high conversion efficiency using MPLC.

In this paper, we designed and fabricated a mode exchange device for data conversion in optical networks and for balancing DMD in long-distance optical fiber communication. In conjunction with the reported research work on MMUX/MDEMUX based on MPLC in our experiment, phase masks are calculated using a wavefront-matching algorithm. The exchange between input modes (LP01, LP11a, LP11b, and LP21) and target modes (LP11a, LP11b, LP21, and LP01) has been realized. The proposed target can be achieved perfectly with only four phase planes, ensuring simulated mode purity larger than 85%, and this process is reversible. The phase structures were fabricated using photolithography and dry-etching processes on a silicon substrate. In the experiment, we integrated the phase planes and FMFs into a unified package. Notably, this device also serves as a broadband photonic component, capable of spanning the C-band and L-band. The mode exchange device has been successfully applied to MDM communication system, realizing the three-channel modes (LP01, LP11, and LP21) multiplexing and data exchange function. 10 Gbit/s OOK signals and QPSK signals have been successfully demonstrated at the wavelength of 1550 nm. The device supports high-performance data exchange based on an MDM optical communications system, further expanding the versatility and applicability of optical networks.

2. Design and Fabrication of the Modes Exchange Device

The modes exchange between multiple coaxial modes, making MDM more balanced during transmission. The modes exchange based on MPLC does not have any mathematical expression. The MPLC is needed to ensure the correspondence between input light field and output light field and modulates the phase shift of the incident light by multiple phase planes. The multiple phase planes are calculated using the wavefront-matching algorithm based on inverse design. The algorithm attempts to match the forward-propagating light field with the backward-propagating light field at any position in space. Thus, the phase distribution of the phase plane is equal to the superposition of the conjugate input light fields and the output light fields in the phase plane. The phase plane is updated by the superposition of the conjugate incident light fields and the output light fields, and the iterative calculation is repeated until the algorithm converges to obtain the multiple phase planes.

Figure 1(a) shows the schematic of modes exchange based on MPLC. The LP01, LP11a, LP11b, and LP21 coaxial modes output from an FMF are exchanged into LP11a, LP11b, LP21, and LP01 coaxial modes when passing through four phase planes. The distance of the incident light field to the first phase plane and the distance between different phase planes are both 20 mm. Figure 1(b) shows the mode exchange sequence. When the LP modes pass through the modes exchange device, LP01 transforms into LP11a, LP11a transforms into LP11b, LP11b transforms into LP21, and LP21 transforms back into

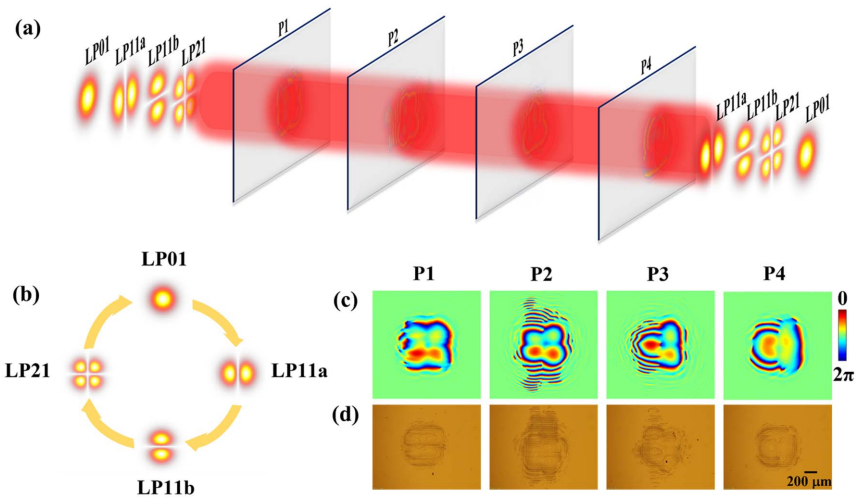

Fig. 1. (a) Schematic of modes exchange; (b) mode exchange sequence between LP01, LP11a, LP11b, and LP21 modes; (c) calculated images of the phase planes; (d) microscopic images of the fabricated phase masks.

LP01 mode, creating a loop. The phase of input (LP01, LP11a, LP11b, and LP21) and target (LP11a, LP11b, LP21, and LP01) light fields are matched by four planes, and phase planes are iteratively updated by the superimposed phases' convergence. To improve the tolerance of the device, a phase-smoothing factor is incorporated into the design to diminish the phase abruptness of the phase planes. Figure 1(c) shows the multiple phase planes obtained by the algorithm convergence. Based on the design, the phase structures are fabricated on a silicon substrate using photolithography and dry-etching processes with an accuracy of 8 μm. The manufactured phase plane is a reflective device with 16 phase levels, ranging from 0 to 2π. The corresponding phase delay was converted to the etching depth of the silicon wafer. Four-time etchings are required with depths of 388, 194, 97, and 48 nm. The etching surface of the phase masks is coated with gold to improve the reflectivity. Figure 1(d) is the microscopic images of the fabricated phase masks, and the fabricated phase structure distributions are close to the calculated images of the phase planes.

3. Experimental Results and Analysis

We experimentally demonstrated the LP modes exchange based on inverse design MPLC devices. In the experiment, we used a reflective phase mask and a mirror to build the MPLC setup, which improved module integration and reduced device insert loss (IL). The LP modes (LP01, LP11a, LP11b, and LP21) are generated by a four-mode multiplexer, which also based on MPLC[11]. The LP modes are output from FMF, collimated by a graded index lens (G-lens), and input to the LP modes exchange device. Four coaxial LP modes are reflected back and forth between the gold-coated phase mask and the mirror, and the exchanged modes are output from the LP modes exchange device and coupled to the FMF by another G-lens. The distance between the phase plane and mirror plane is 9.8 mm. The waist diameter of the input beam and output beam is 300 μm. The schematic diagram of the reflective mode exchange device is shown in Fig. 2(a), and the captured physical image is depicted in Fig. 2(b). The IL of the device includes mode conversion loss and reflection loss between the phase plane and mirror. Here, the IL is defined as

$$\mathrm{IL} = 10\ \log\left(\frac{P_{\mathrm{out}}}{P_{\mathrm{in}}}\right), \tag{1}$$

where P_{out} is the measured output power of the exchanged mode, and P_{in} is the power of the input beam. The mode intensity profile and phase distribution of the simulated output modes are shown in Figs. 2(c) and 2(d). In the experiment, the calculated device IL is lower than 2.2 dB. The intensity distributions of LP modes exchanged within free space were imaged at the wavelength of 1550 nm, as shown in Fig. 2(e). The output modes were measured using Fourier transform interferometry, and the intensities and phases can be reconstructed using digital holography, as illustrated in Fig. 2(f). These experimental results

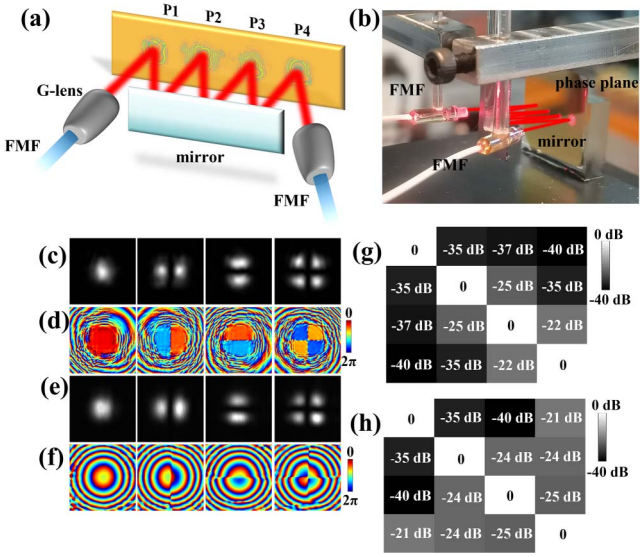

Fig. 2. (a) Schematic diagram of the reflective mode exchange device; (b) physical image of the device; (c) intensity distribution of the calculated modes; (d) phase distribution of the calculated modes; (e) intensity distribution of the generated modes by the modes exchange device; (f) phase distribution of the reconstructed modes; (g) calculated and (h) experimental mode crosstalk gray matrices.

are basically consistent with the calculated results. Over the past few decades, WDM has played an important role in increasing fiber communication capacity. The efficient combination of WDM and MDM can further expand the capacity of optical fiber communication. We also observed the conversion efficiency of the LP modes exchange device at different wavelengths, covering the C-band and L-band, as shown in Fig. 3. The variation in conversion efficiency is lower than 16%, indicating that the device is a broadband photonic device. Some modes exhibit significant IL fluctuations, which may be attributed to alignment errors during the experiment.

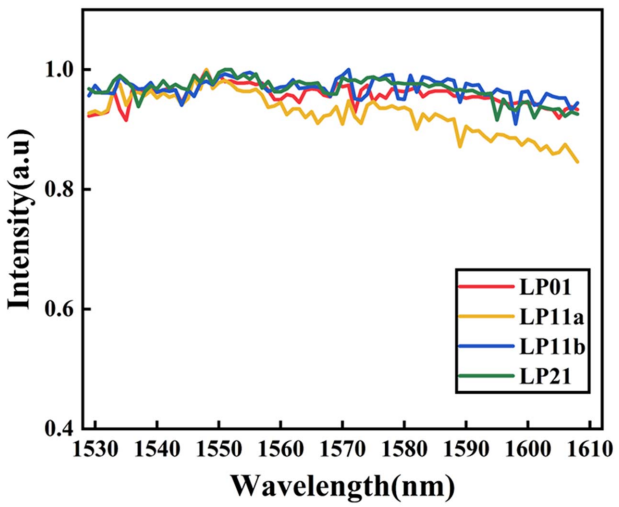

Fig. 3. Conversion efficiency of the mode exchange device over the C-band and the L-band wavelengths.

The mode crosstalk is a phenomenon where different modes interfere with each other and is characterized by the mode crosstalk matrix. The crosstalk between mode m and mode n is defined as

$$\text{Crosstalk}_{m,n} = 10\ \log\left(\frac{P_m}{P_n}\right), \tag{2}$$

where P_m is the measured power of the target mode, and P_n is the measured unnecessary power. The calculated and experimental mode crosstalk matrices are extracted, as shown in Figs. 2(g) and 2(h), respectively. The experimental values are less than −21 dB and slightly larger than the calculated values, which is mainly due to imperfect fabrication and misalignment.

To evaluate the data transmission performances of the mode exchange device, a back-to-back MDM system based on an MMUX, 2 m FMF, and an MDEMUX was characterized for data exchange, as shown in Fig. 4(a). However, LP11a and LP11b modes in the same group within FMF are degenerated modes. They are prone to strong coupling, which affects the effectiveness of communication. Therefore, the LP01, LP11b, and LP21 modes are selected as the three channels for transmission. 10 Gbit/s OOK fundamental mode light signals at the wavelength of 1550 nm generated independently using standard optical transceivers were divided into three groups. The MMUX multiplexed them into the coaxial multimode light signals and then coupled them into FMF. After the transmission of FMF, a mode exchange device is used for data conversion. Finally, the light signals were demultiplexed into three channel fundamental mode light signals by MDEMUX and then detected by the transceiver of the corresponding input channel. The direct detection technique is selected to reduce cost and system complexity. By measuring the input power and output power of the system, the system mode crosstalk gray matrices are obtained, as illustrated in Fig. 4(b), which are below −6.6 dB. The detected power ranged from −17 to −32 dBm with an interval of 1 dB. ILs and the mode crosstalk are the main factors affecting the signal-to-noise ratio (SNR) in the MDM communication system, with a reduced optical module detection sensitivity to −32 dBm. As shown in Fig. 4(c), the bit error rate (BER) increases as the received power decreases, and the BERs for all channels remain below the FEC threshold of 3.8×10^{-3}. It is obvious that error-free transmission can be achieved with pre-equalization.

For visualization purposes, we also measured the constellation diagrams of three channels (LP01, LP11b, and LP21) carrying 10 Gbit/s QPSK signals. As shown in Figs. 4(d)–4(f), the constellation diagram for the LP21 mode appears slightly more dispersed compared to the other two modes, primarily due to lower received power. The calculated Q-factor exceeds 6.94,

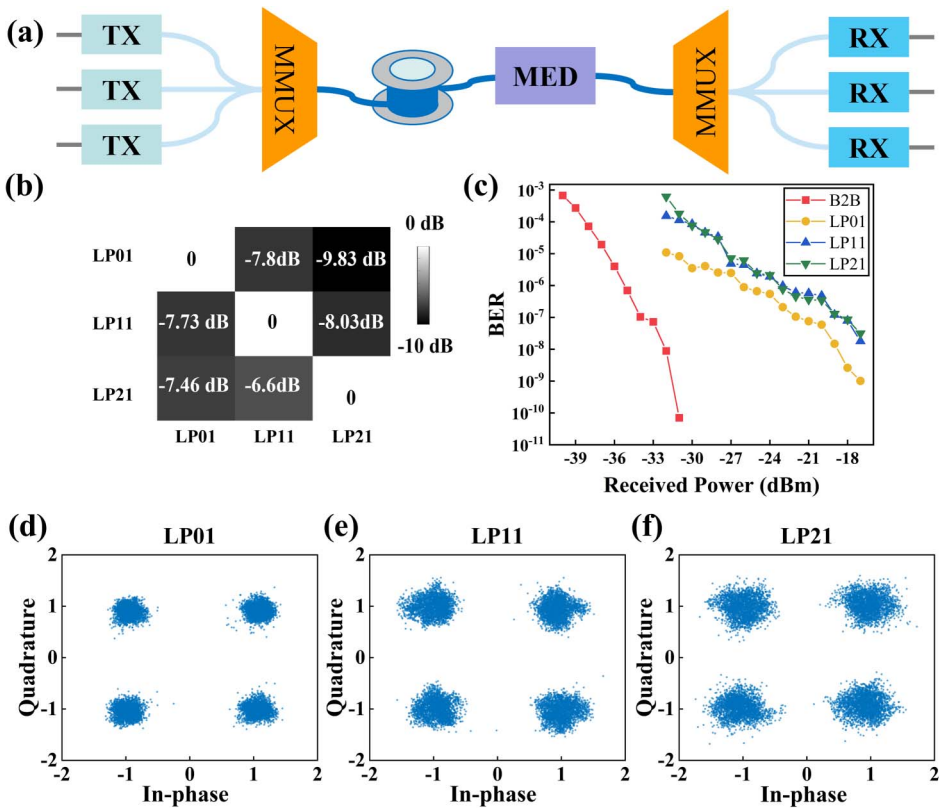

Fig. 4. (a) Experimental setup of the few-mode optical fiber communication system based on mode exchange device; (b) measured mode crosstalk gray matrices of the communication system; (c) measured BER characteristics of the system. Constellation diagrams of the QPSK signals: (d) LP01 mode; (e) LP11 mode; (f) LP21 mode.

which can be further optimized using communication algorithms. Utilizing the G-lens for multimode lights coupling into the FMF during transmission, coupling loss also emerges as a primary contributor to system losses. The combination of mode exchange devices with the MDM communication system enhances the flexibility of optical communication networks. In future research, optimizing the coupling loss and system crosstalk will enable the device to support transmission in long-distance communication.

4. Conclusion

In this paper, we designed and fabricated a mode exchange device for data conversion using MPLC technology in optical networks. The device supports the conversion between input modes (LP01, LP11a, LP11b, and LP21) and target modes (LP11a, LP11b, LP21, and LP01). The mode exchange device has been demonstrated in the MDM communication system. It is worth noting that the method for designing and fabricating the device is scalable. We can configure various input and output mode arrangements to calculate and process different phase structures, thereby enhancing the flexibility of mode conversion. We have demonstrated mode conversion for four modes, and we can showcase mode exchanges for higher-order modes in the future, such as 6-modes or 10-modes. Additionally, we can increase the integration of the device using metasurface technology. The device has exhibited excellent performance in the wideband test, enabling the establishment of the WDM-SDM hybrid systems to enhance communication capacity. Overall, the combination of the mode exchange device, MMUXs/MDEMUXs, and FMFs further increases the capacity of communication systems and enriches the functionality of optical networks.

Acknowledgements

This work was supported by the Guangdong Major Project of Basic Research (No. 2020B0301030009), the National Natural Science Foundation of China (Nos. U23A20372, 61935013, 62105215, and 62275171), the Shenzhen Peacock Plan (No. KQTD20170330110444030), the Stable Support Project of Shenzhen (Nos. 20220810152651001 and 20220811103827001), the Natural Science Foundation of Guangdong Province (Nos. 2020A1515011185 and 2022A1515011642), and Shenzhen University (No. 2019075).

References

1. P. J. Winzer, D. T. Neilson, and A. R. Chraplyvy, "Fiber-optic transmission and networking: the previous 20 and the next 20 years [Invited]," Opt. Express **26**, 24190 (2018).
2. C. T. Xu, B. H. Liu, C. Peng, *et al.*, "Heliconical cholesterics endows spatial phase modulator with an electrically customizable working band," Adv. Opt. Mater. **10**, 2201088 (2022).
3. Z. Wei, A. Kong, J. Hu, *et al.*, "Parallel arrayed waveguide grating for wavelength-mode hybrid multiplexing," Opt. Lett. **47**, 4311 (2022).
4. S. Okamoto, K. Minoguchi, F. Hamaoka, *et al.*, "A study on the effect of ultra-wide band WDM on optical transmission systems," J. Lightwave. Tech. **38**, 1061 (2020).
5. A. G. Alharbi, M. J. O. Singh, and Q. Electronics, "Downstream performance evaluation of a 4 × 112 Gbps hybrid wavelength-polarization division multiplexed next generation-passive optical network," Opt. Quantum Electron. **54**, 384 (2022).
6. J. Liu, J. Zhang, J. Liu, *et al.*, "1-Pbps orbital angular momentum fibre-optic transmission," Light Sci. Appl. **11**, 202 (2022).
7. A. E. Willner, Z. Zhao, C. Liu, *et al.*, "Perspectives on advances in high-capacity, free-space communications using multiplexing of orbital-angular-momentum beams," APL Photonics **6**, 28 (2021).
8. D. J. Richardson, J. M. Fini, and L. Nelson, "Space-division multiplexing in optical fibres," Nat. Photonics **7**, 354 (2013).
9. J. Wang, J.-Y. Yang, I. M. Fazal, *et al.*, "Terabit free-space data transmission employing orbital angular momentum multiplexing," Nat. Photonics **6**, 488 (2012).
10. L. Wang, R. M. Nejad, A. Corsi, *et al.*, "Linearly polarized vector modes: enabling MIMO-free mode-division multiplexing," Opt. Express **25**, 11736 (2017).
11. J. Fang, J. Bu, J. Li, *et al.*, "Performance optimization of multi-plane light conversion (MPLC) mode multiplexer by error tolerance analysis," Opt. Express **29**, 37852 (2021).
12. H. Cao, Y. Liang, L. Wang, *et al.*, "Efficient dense orbital angular momentum demultiplexing enabled by quasi-wavelet conformal mapping," Laser Photonics Rev. **17**, 2200631 (2023).
13. C. T. Xu, D. W. Zhang, R. Yuan, *et al.*, "Optical orbital angular momentum processors with electrically tailored working bands," Laser Photonics Rev. **17**, 2201013 (2023).
14. G. Li, J. Rho, and X.-C. Yuan, "Optical orbital angular momentum: thirty years and counting," Adv. Photonics **5**, 030101 (2023).
15. N. K. Fontaine, J. Carpenter, S. Gross, *et al.*, "Photonic lanterns, 3-D waveguides, multiplane light conversion, and other components that enable space-division multiplexing," Proc. IEEE **110**, 1821 (2022).
16. N. Mahadzir, A. Amphawan, T. Masunda, *et al.*, "Tapered waveguide design for mode conversion in mode division multiplexing (MDM)," Proc. IEEE **41**, 448 (2021).
17. Q. Mai, C. Wang, X. Wang, *et al.*, "Metasurface based optical orbital angular momentum multiplexing for 100 GHz radio over fiber communication," J. Lightwave. Tech. **39**, 6159 (2021).
18. R. Yuan, C. T. Xu, H. Cao, *et al.*, "Spin-decoupled transflective spatial light modulations enabled by a piecewise-twisted anisotropic monolayer," Adv. Sci. **9**, 2202424 (2022).
19. S. Zhang, A. Okamoto, T. Shiba, *et al.*, "Spatial mode exchange technique using volume holograms with a random optical diffuser for reduction of crosstalk," Opt. Rev. **28**, 181 (2021).
20. H. Jia, T. Zhou, X. Fu, *et al.*, "Inverse-design and demonstration of ultracompact silicon meta-structure mode exchange device," ACS Photonics **5**, 1833 (2018).
21. S. Chen, W. Liu, Z. Li, *et al.*, "Metasurface-empowered optical multiplexing and multifunction," Adv. Mater. **32**, 1805912 (2020).
22. L. Deng, Y. Xu, R. Jin, *et al.*, "On-demand mode conversion and wavefront shaping via on-chip metasurfaces," Adv. Opt. Mater. **10**, 2200910 (2022).
23. S. Zhang, A. Okamoto, T. Shiba, *et al.*, "Spatial mode exchange technique using volume holograms with a random optical diffuser for reduction of crosstalk," Opt. Rev. **28**, 181 (2021).
24. G. Labroille, B. Denolle, P. Jian, *et al.*, "Efficient and mode selective spatial mode multiplexer based on multi-plane light conversion," Opt. Express **22**, 15599 (2014).
25. N. K. Fontaine, R. Ryf, H. Chen, *et al.*, "Laguerre-Gaussian mode sorter," Nat. Commun. **10**, 1865 (2019).
26. J. Fang, L. I. Jinpei, A. Kong, *et al.*, "Optical orbital angular momentum multiplexing communication via inversely-designed multiphase plane light conversion," Photonics Res. **10**, 2015 (2022).
27. H. Wen, H. Liu, Y. Zhang, *et al.*, "Scalable Hermite–Gaussian mode-demultiplexing hybrids," Opt. Lett. **45**, 2219 (2020).
28. A. R. Kong, T. Lei, J. C. Fang, *et al.*, "Achromatic broadband multi-layer diffraction mode multiplexing," Laser Photonics Rev. **17**, 2200845 (2023).